JOURNAL OF FUNCTIONAL FOODS 14 (2015) 23–32

Available online at www.sciencedirect.com

ScienceDirect

journal homepage: www.elsevier.com/locate/jff

Structure, antioxidant and α-amylase inhibitory activities of longan pericarp proanthocyanidins

Caili Fu [a,b], *Xuena Yang* [b], *Shaojuan Lai* [c], *Chang Liu* [b], *Shangrong Huang* [b], *Hongshun Yang* [a,d,*]

[a] *Food Science and Technology Programme, c/o Department of Chemistry, National University of Singapore, 3 Science Drive 3, Singapore 117543, Republic of Singapore*

[b] *College of Bioscience & Biotechnology, Fuzhou University, Fuzhou 350108, China*

[c] *College of Biological Engineering, Henan University of Technology, Zhengzhou, Henan 450052, China*

[d] *National University of Singapore (Suzhou) Research Institute, 377 Lin Quan Street, Suzhou Industrial Park, Suzhou, Jiangsu 215123, China*

ARTICLE INFO

Article history:
Received 20 November 2014
Received in revised form 22 January 2015
Accepted 22 January 2015
Available online

Keywords:
Longan
Pericarp
Proanthocyanidins
Antioxidant activity
α-Amylase inhibitor
Structure

ABSTRACT

Longan pericarp proanthocyanidins (LPPs) were extracted and examined by structural and bioactive analyses. By ^{1}H and ^{13}C NMR spectra, LPPs were identified for the first time containing dominant catechin/epicatechin units with a mean degree of polymerisation of 3.3. Consistent with this result, electron spray ionisation (ESI) mass spectra revealed that the predominant LPPs were poly(epi)catechin with abundant A-type and B-type linkages. Matrix-assisted laser desorption ionisation time of flight (MALDI-TOF) mass spectra of LPPs showed dominant $[M + Na]^+$ peaks that corresponded to procyanidin trimers–octamers. The presence of galloyl group in monomeric units of LPPs was confirmed by FT-IR, NMR, ESI and MALDI-TOF mass spectrometry (MS). Moreover, LPPs had a strong antioxidant activity of 1.23×10^4 μmol TE/g as measured by oxygen radical scavenging capacity (ORAC), and α-amylase inhibitory activity with IC_{50} for uncompetitive α-amylase inhibition of 0.075 mg/mL. These results indicate LPPs are promising antioxidant which could be applied as potential functional food components.

1. Introduction

Longan (*Dimocarpus longan* Lour.) is a tropical/subtropical fruit belonging to Sapindaceae family and is broadly produced in China, Thailand, India, and some other Southeast Asia countries (Yang, Jiang, Shi, Chen, & Ashraf, 2011). Longan fruit has desirable flavour and is used as a widely accessible source of tonic food. The edible portion of longan is semi-translucent to white, whereas the leathery and indehiscent pericarp, which accounts for approximately 15–20% of the whole fruit weight, usually is discarded as an agricultural waste (Prasad et al., 2010; Yang et al., 2011).

Longan pericarps are rich of bioactive compounds including significant amounts of phenolic compounds and polysaccharides, which can potentially be applied in chronic disease prevention or as functional food components (Jaitrong, Rattanapanone, & Manthey, 2006; Panyathep, Chewonarin, Taneyhill, Surh, & Vinitketkumnuen, 2013; Prasad et al., 2009, 2010; Yang, Zhao, & Jiang, 2009). Proanthocyanidins, one of the

* *Corresponding author*. Department of Chemistry, Food Science and Technology Programme, National University of Singapore, 3 Science Drive 3, Singapore 117543, Singapore. Tel.: +65 65164695; fax: +65 67757895.
E-mail address: chmynghs@nus.edu.sg (H. Yang).

Chemical compounds studied in this article: Procyanidin trimer (PubChem CID 169853); Procyanidin dimer (PubChem CID 122738); Trolox (PubChem CID 40634).

http://dx.doi.org/10.1016/j.jff.2015.01.041
1756-4646/

most abundant type of natural phenolic compounds, possess several bioactivities and occur in many fruits and vegetables (Lei, Ren, Chen, Liu, & Ruan, 2014; Nagahama et al., 2014; Neto, 2007; Ou & Gu, 2014; Wangensteen et al., 2014; Zou et al., 2014). For example, proanthocyanidins from cranberry were able to prevent cancer, lower the risk of urinary tract infection and scavenge reactive oxygen species (ROS) (Neto, 2007). Apple proanthocyanidins can improve the anti-carcinogenic attributes of lysosomotropic compounds (Seiler et al., 2006). In addition, proanthocyanidins from many plants have antioxidant activities (Fu, Loo, Chia, & Huang, 2007; Huang, Ou, Hampsch-Woodill, & Flanagan, 2002; Shao et al., 2004). Synergistic effect of different plant proanthocyanidins on scavenging ROS has been reported (Shao et al., 2004). Besides antioxidant activity, proanthocyanidins possess potentially positive effects on glycaemic control, as indicated by their strong inhibitory capability on pancreatic α-amylase, thus proanthocyanidins may be used for the long-term treatment for type II diabetes mellitus (DM) (Hargrove, Greenspan, Hartle, & Dowd, 2011; Wang, Liu, Song, & Huang, 2012).

Longan pericarps have also been reported to contain proanthocyanidins (He et al., 2009). To the best of our knowledge, the comprehensive information about structural profile and bioactivity of longan pericarp proanthocyanidins (LPPs) is not clear. The aim of the current study was to isolate LPPs from longan pericarps and characterise their structures and bioactivity. The structures were examined by ultraviolet/visible (UV/vis) spectrophotometry, Fourier transform infrared spectroscopy (FT-IR), nuclear magnetic resonance (NMR), electron spray ionisation (ESI)–mass spectrometry (MS), and matrix-assisted laser desorption/ionisation time of flight (MALDI-TOF)–MS. The peroxyl radical scavenging capacity and α-amylase inhibition activity of LPPs were tested by oxygen radical absorbance capacity (ORAC) assay and kinetic analysis, respectively.

2. Materials and Methods

2.1. *Materials and reagents*

Longan (cultivar "Si Chomphu", cultivated in Thailand) was purchased from a local market and transferred to the laboratory within 2 h. The moisture content of longan pericarps was determined by weighing the weight changes of a certain amount of fresh pericarps using a moisture analyser. Proanthocyanidin extracts of commercial grape seed (95% purity) were obtained from Chengdu SanHerb Plant Extract Co. Ltd. (Chengdu, Sichuan, China). All solvents used were of analytical grade unless otherwise specified. Sephadex™ LH-20 was purchased from GE Healthcare Bio-Sciences AB (Uppsala, Sweden). The compounds 2, 5-dihydroxybenzoic acid, 3, 5-dinitrosalicylic acid, potassium sodium tartrate tetrahydrate, 2, 2′-azobis (2-amidinopropane) dihydrochloride, fluorescein disodium salt, α-amylase (EC 3.2.1.1) and Trolox were purchased from Sigma-Aldrich Chemical Company (St. Louis, MO, USA).

2.2. *Extraction and purification of LPPs*

The overall extraction and purification flow diagram of LPPs is shown in Figure 1A. The meshed longan pericarps were sieved and the powder (2.0 kg) with particle size smaller than 600 μm was soxhlet defatted three times, each time with 1200 mL hexane. Subsequently, proanthocyanidin fractions were extracted from the residue by mixed solution of acetone/water (7:3, v/v, three times, each time with 4000 mL) for 4 h, according to a previous method (Fu et al., 2007). Then the mixture was filtered and acetone in the filtrate was removed by a rotary evaporator set at 40 °C. The extraction procedure was repeated two times and the produced water layer was pooled, and centrifuged at 3000 *g* for 20 min. The supernatant was collected and liquid–liquid extracted with chloromethane (two times, each time with 500 mL) to remove lipophilic compounds. The water phase was concentrated to about 60 mL and filtered through a filter (45 μm porosity, Minisart) before loading on a Sephadex LH-20 column (50 g Sephadex LH-20, equilibrated with methanol/water (1:1, v/v) for 3 h). The column was then washed with 1000 mL methanol/water (1:1, v/v) to remove carbohydrates and other matters. The adsorbed LPPs were recovered by eluting with 500 mL 70% (v/v) aqueous acetone. Acetone was removed using a rotary evaporator at 40 °C.

2.3. *Structural analyses*

The purified LPPs were characterised using UV/vis, FT-IR and ^{1}H and ^{13}C NMR spectroscopy, ESI–mass spectrometry (MS), and MALDI-TOF–MS. UV/vis spectra were recorded in the range from 200 to 700 nm, with a quartz cuvette (1 cm path length). FT-IR spectra of the KBr samples of LPPs were scanned between 4000 and 400 cm^{-1} and then recorded in the transmission mode adopting a Spectrum One FTIR spectrometer (PerkinElmer, Waltham, MA, USA). ^{1}H and ^{13}C NMR spectra were recorded in deuterated methanol at 300 MHz for ^{1}H and 75 MHz for ^{13}C with a Bruker AC300 spectrometer (Bruker BioSpin GmbH, Silberstreifen, Rheinstetten, Germany) while chemical shifts were recorded on a δ (ppm) scale. The ESI mass spectra were collected from a Finnigan/MAT LCQ ion trap mass spectrometer (Thermo-Finnigan, San Jose, CA, USA) with full-scan mass spectra from m/z 50 to 2000, using a negative ion mode with a scan speed of 1 s per scan. The heated capillary and voltage were kept at 250 °C and 4.5 kV, respectively. During the test, nitrogen was operated at 20 psi for auxiliary gas flow rate and 80 psi for sheath gas flow rate. MALDI-TOF mass spectra were obtained on a Voyager-DE STR mass spectrometer (Applied Biosystems, Foster City, CA, USA) equipped with delayed extraction and a N_2 laser set at 337 nm. The measurements were performed under the conditions: 21 kV acceleration voltage in linear flight path, positive polarity, 100 pulses per spectrum and 3 ns for the length of one laser pulse. The LPPs were dissolved in methanol for both ESI–MS and MALDI-TOF–MS. Sodium chloride (0.1 M aqueous solution) and 2, 5-dihydroxybenzoic acid (10 mg/mL) as matrix were used to increase ion formation (Behrens, Maie, Knicker, & Kögel-Knabner, 2003).

2.4. *Antioxidant capacity analysis*

Oxygen radical absorbance capacity (ORAC) assay was carried out with a Synergy HT fluorescent microplate reader (Bio-tek Instruments Inc., Winooski, VT, USA), according to Huang et al. (2002). An excitation wavelength of 485 nm and an emission wavelength of 530 nm were adopted and the ORAC data were

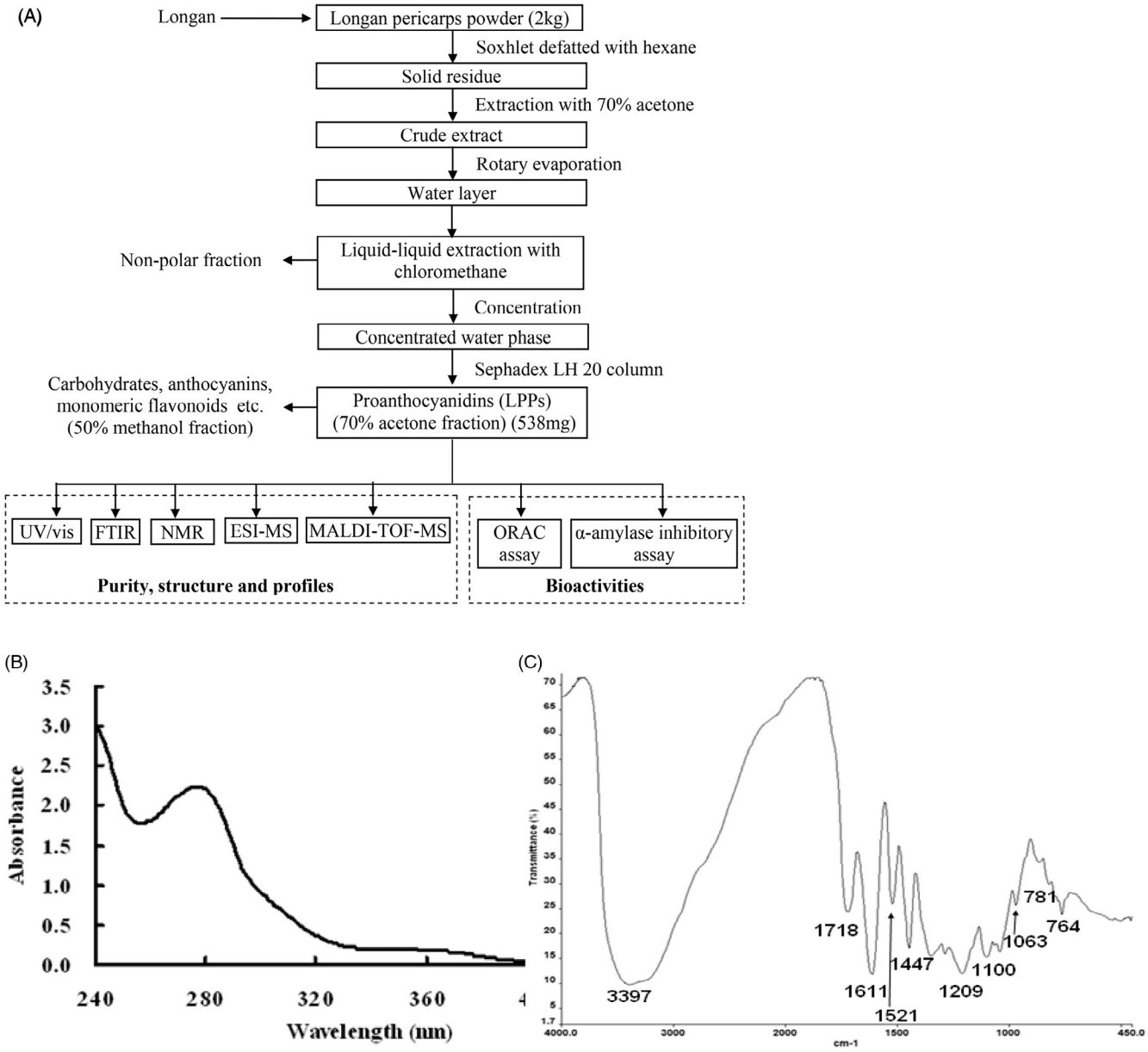

Fig. 1 – Procedure flow chart and UV/vis as well as FT-IR spectra of longan pericarp proanthocyanidins (LPPs). (A) Flow chart illustrating the procedures for extracting and purifying LPPs; (B) UV/vis spectrum of LPPs; C. FT-IR spectrum of LPPs.

expressed as micromoles of Trolox equivalents per gram (μmol TE/g).

2.5. *α-Amylase inhibition assay*

The α-amylase inhibitory activities of LPPs were determined by the method of Ranilla, Kwon, Apostolidis, and Shetty (2010) with slight modification. LPPs were dissolved in 50% ethanol to achieve a 5 mg/mL of sample solution which was further diluted with 0.02 M sodium phosphate buffer to produce working solutions of various concentrations. α-Amylase solution (0.25 mL, 0.075 mg/mL, dissolved in 0.02 M sodium phosphate buffer, pH 6.9 with 6.7 mM NaCl) was mixed with 0.25 mL of sample solution of various concentrations. The mixture was incubated at 37 °C for 10 min. After pre-incubation, 0.5 mL of 1% (w/w) starch solution in 0.02 M sodium phosphate buffer (pH 6.9 with 6.7 mM NaCl) was added, and the mixture was incubated at 37 °C for 3 min. The reaction was stopped by adding 1.0 mL of dinitrosalicylic acid colour reagent. The test tubes were placed in a boiling water bath and incubated for 8 min followed by cooling to room temperature. Then, the reaction mixture was diluted with 10 mL distilled water, and the absorbance was recorded at 540 nm. The absorbance of sample blanks (buffer only) and a control (buffer in place of sample extract) were measured as well. The α-amylase inhibitory activity was calculated according to the following equation:

$$\%inhibition = \frac{A_1 - (A_2 - A_3)}{A_1} \times 100\% \quad (1)$$

where A_1 was the absorbance of control, A_2 was the absorbance of sample and A_3 was the absorbance of sample blanks.

The type of inhibition was determined by kinetics curve and the Lineweaver–Burk plot (Hargrove et al., 2011). The α-amylase solution (0.25 mL, 0.075 mg/mL, dissolved in 0.02 M PBS, pH 6.9 with 6.7 mM NaCl) was mixed with sample solution (0.25 mL, 0.025 mg/mL, dissolved in 0.02 M PBS, pH 6.9 with 6.7 mM NaCl), and 0.5 mL of substrate solution at various concentrations. The absorbance was then read at 540 nm.

2.6. Statistical analysis

All assays were performed in triplicate. The results were expressed as mean ± SD (standard deviation). Significance of differences was determined using Duncan's multiple range test by SAS software (version 9.2, Cary, NC, USA). Comparisons that yielded $P < 0.05$ were considered significant.

3. Results and discussion

3.1. UV/vis and FT-IR analysis of LPPs

The yield of LPPs was 538 mg from 2.0 kg of fresh longan pericarps, which accounts for 0.005% of total fresh fruit weight (Table 1). The LPPs were freeze-dried for 3 days and the powder (light brown) with particle size smaller than 250 μm was obtained. The yield of dried LPPs corresponded to 70 mg proanthocyanidins per 100 g dry pericarps and agreed with a previous report (He et al., 2009). Here in the current study, the LPPs were purified by chromatographic separation with Sephadex-LH 20 column, a technique that had been successfully used for the purification of proanthocyanidins from different plants (Chen et al., 2014; Fu et al., 2007; Wang et al., 2012; Zhou, Lin, Wei, & Tam, 2011). UV/vis spectra proved that pure proanthocyanidin fractions were eluted from chromatographic column in the same way, since the purified LPPs showed a catechin-like and symmetrical peak near 280 nm (Fig. 1B), which is a typical characteristic of proanthocyanidins (Chen et al., 2014; Zhou et al., 2011). The peak at 280 nm for LPPs was consistent with proanthocyanidins from *Pinus radiata* bark though minor differences were found in low wavelength regions (Ku & Mun, 2007).

Table 1 – ORAC values and IC_{50} for α-amylase inhibition of proanthocyanidins.

	LPs	LPPs	cGSPs
Percent of fruit weight (%)	16.8 ± 0.3	0.005	–
Moisture content (%)	61.5 ± 2.6	0	–
Yield (%)	–	0.07	–
mDP	–	3.3	–
IC_{50} for α-amylase inhibition (mg/ml)	–	0.075 ± 0.003	–
ORAC value ($\times 10^4$ μmol TE/g)	–	1.23 ± 0.02	1.01 ± 0.09

LPs, longan pericarps; LPPs, longan pericarp proanthocyanidins; cGSPs, commercial grape seed proanthocyanidins; mDP, mean degree of polymerisation; yield, dry matter against longan pericarps; ORAC, oxygen radical absorbance capacity.

In FTIR spectrum of LPPs, peaks at 3397, 1718, 1611, 1521, 1447, 1209, 1100, 1063, 781 and 764 cm^{-1} were clearly observed (Fig. 1C). More specifically, the band at 3397 cm^{-1} was corresponding to —OH stretch vibration in the phenolic structure of LPPs. Band at 1718 cm^{-1} may be due to the stretching vibration of C═O, suggesting that the presence of galloyl group (Ku & Mun, 2007; Yazaki & Hillis 1977). Bands at 1521 and 1447 cm^{-1} were assigned to the aromatic structure of LPPs. Peaks at 1521 and 781 cm^{-1} were generally attributed to the aromatic ring breathing manner. The band at 1447 cm^{-1} corresponded to —CH deformation while aromatic ring vibration appeared at 1209 cm^{-1}. When identifying proanthocyanidins, it is helpful to further explore bioactivities and structure–bioactivity relationship to know the subclass of proanthocyanidins. The proanthocyanidins consisting exclusively of (epi)catechin are designated as procyanidin (PC). While prodelphinidin (PD) is another subclass of proanthocyanidins, which contains (epi)gallocatechin as subunits. Bands at 764 and 730 cm^{-1} were attributed to CH out-of-plane conformations in PC and PD, respectively. The strong absorption bands were 3397, 1611, 1521 and 1209 cm^{-1}, which may be caused by the representative functional groups of LPPs (Ku & Mun, 2007; Xu, Zou, Yang, Yao, & Li, 2012; Yazaki & Hillis, 1977), indicating the main presence of procyanidin (PC) structure (Foo, 1981; Ku & Mun, 2007; Yazaki & Hillis, 1977). Because band at 764 cm^{-1} was much stronger than band at 730 cm^{-1}, thus LPPs contained mainly PC but small amount of PD units (Ku & Mun, 2007).

3.2. NMR analysis of LPPs

^1H NMR spectrum of LPPs is shown in Fig. 2. It presents B-ring proton signals (H-2′, 5′ and 6′) at 6.5–7.8 ppm and A-ring proton signals (H–6 and 8) at 5.8 and 6.5 ppm together with the H4 signals in the terminal units at 2.4–3.0 ppm. The mean degree of polymerisation (mDP) of LPPs was obtained by calculating the integrated value of the A-ring proton signals and the intensity of the H4 signals based on Equation (2) (Guyot, Le Guerneve, Marnet, & Drilleau, 1999). As a result, the mDP of the LPPs was 3.3, suggesting LPPs were oligomeric proanthocyanidins which possessed higher absorption rate than polymers with higher mDP (Ou & Gu, 2014).

$$mDP = 2 \times \frac{(H-6+H-8)\ \text{signal area}}{(H-4)\ \text{signal area}} - 1 \quad (2)$$

Since ^{13}C NMR spectrum was able to elucidate the large amount of structural information including the monomeric units, the stereochemistry of the heterocyclic ring (C2═C3), and the type of interflavan linkage according to reports from different research groups (Chen et al., 2014; Czochanska, Foo, Newman, & Porter, 1980; Ku & Mun, 2007; Wang et al., 2012), LPPs were next examined by ^{13}C NMR. Figure 3 shows the ^{13}C NMR spectrum of the LPPs in methanol-d_4. The characteristic ^{13}C peaks in LPPs were corresponding to a dominant amount of PC oligomers while no peaks of non-proanthocyanidin impurity were observed. Thus, the purity of the LPPs was also confirmed by ^{13}C NMR spectrum, which indicated the absence of non-proanthocyanidin impurity (Fig. 3). As regards the subclass of proanthocyanidins, a minor amount of PDs was also

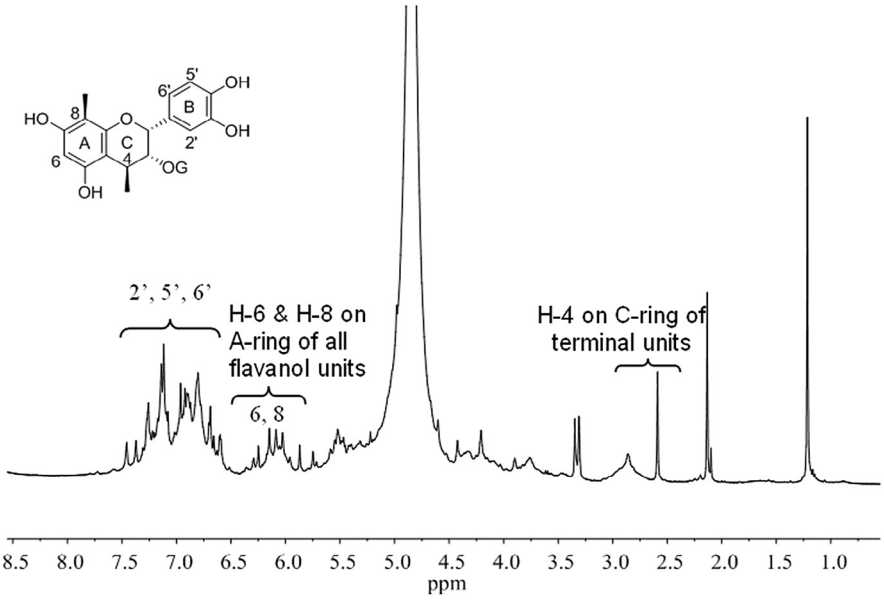

Fig. 2 – ^{1}H NMR spectrum of longan pericarp proanthocyanidins (LPPs) (room temperature, 300 MHz, solvent, CD_3OD).

present besides dominant PCs. The C4′ peak of PDs was observed at 131 ppm, overlapping with the chemical shifts of C1′ (PC). These data suggest LPPs contained a dominant amount of PC units as well as a minor amount of PDs and are consistent with the result of FT-IR spectrum for LPPs.

^{13}C NMR spectrum also provided the structural diversity of the linkage (A and B types) and stereoisomer of monomeric units of PCs and PDs. In particular, C5, C7, C4′ and C8a carbons of PC emerged at 160–150 ppm. There were peaks at 145.3 and 145.5 ppm, corresponding to C3′ and C4′ of PC units, respectively (Czochanska et al., 1980). The clusters of peaks between 110 and 90 ppm were assigned to C8 and C6 of PC, C6′ (PD) and C2′ (PD). Furthermore, the ratio of the 2, 3-*cis* to 2, 3-*trans* isomers could be measured through the distinct differences in their respective C2 chemical shifts by detecting the region between 70 and 90 ppm which was sensitive to the stereochemistry of the C-ring (Czochanska et al., 1980; Fu et al., 2007). For both *cis* and *trans* isomers, C3 occurred at 71.4 ppm while C2 showed a resonance at 75.3 ppm and 79 ppm for the *cis* form and the *trans* form, respectively. From the peak areas for C2, it was concluded that the ratio of *trans* isomers was approximately equal to that of *cis* isomers in LPPs.

The C4s of the extension units exhibited an extensive peak at 36 ppm while the terminal C4 showed multiple lines at 29 and 27 ppm. The presence of galloyl group, which is revealed by FT-IR spectrum of LPPs, was confirmed by the signal of C3″, C4″ and C5″ appearing at 131 ppm together with carbonyl carbon peaks occurring above 165 ppm. The presence of signals at 151–152 ppm owing to C5 and C7 of the A-ring indicated that there were some A-type linkages. This indication was supported by the additional bond observed at 104.7 ppm which suggested the chemical shift of the ketal carbon (C2). Overall, the results discussed earlier are consistent with previous reports (Czochanska et al., 1980; Fu, Wang, Ng, Song, & Huang, 2013).

3.3. *ESI and MALDI-TOF–mass spectra of LPPs*

Although the information from ^{13}C NMR spectrum suggests LPPs contain a complex typical structure of proanthocyanidins, it could not provide the quantitative data related to the structural proanthocyanidins profile as determined by ESI or MALDI-TOF–mass spectrometry (MS). Thus, ESI–MS analysis was carried out to further characterise LPPs.

Figure 4A shows the ESI–MS spectrum of the LPPs recorded in the negative ion mode. According to the peak signals, a first series of abundant ions separated by 288 Da were observed from *m*/*z* 577 to 1905, which corresponded to the molecular masses of LPPs with DP 2–6, suggesting that the dominant species were oligomeric PCs. This observation agreed well with the data obtained from ^{1}H and ^{13}C NMR spectra. Peak at *m*/*z* 432 could be caused by the fragmentation of propelargonidin dimer (*m*/*z* 559) after heterocyclic ring fission (HRF) (Gu et al., 2003). A 1, 3, 5-trihydroxybenzene (molecular weight of 126 Da) structure in A-ring of the extension unit maybe present according to the loss of 126 Da (i.e. 559–432) in the HRF pathway. For LPPs, A-type PC trimer (*m*/*z* 863) was the most abundant followed by B-type PC trimer (*m*/*z* 865) and dimmer (*m*/*z* 577) although other less intense signals were also observed in the higher *m*/*z* values. When there is an A-type interflavan linkage between adjacent flavan-3-ol subunits, two hydrogen atoms (Δ2 amu) are lost to format this (4β-8, 2β-O-7) interflavan bond. ESI–MS spectrum of LPPs shows several A-type proanthocyanidins such as trimer (*m*/*z* 863) and hexamer (m/z 1905) that were two units less than B-type trimeric and hexameric PCs. PC dimer gallate (m/z 729) and PD hexamer gallate (m/z 1905) appeared with less abundant signals, which is consistent with the NMR results. Interestingly, the peak at *m*/*z* 1009 had 144 mass units more than trimer ion (*m*/*z* 865) and lower than tetramer (*m*/*z* 1153), which might be due to the doubly charged species of heptameric PCs.

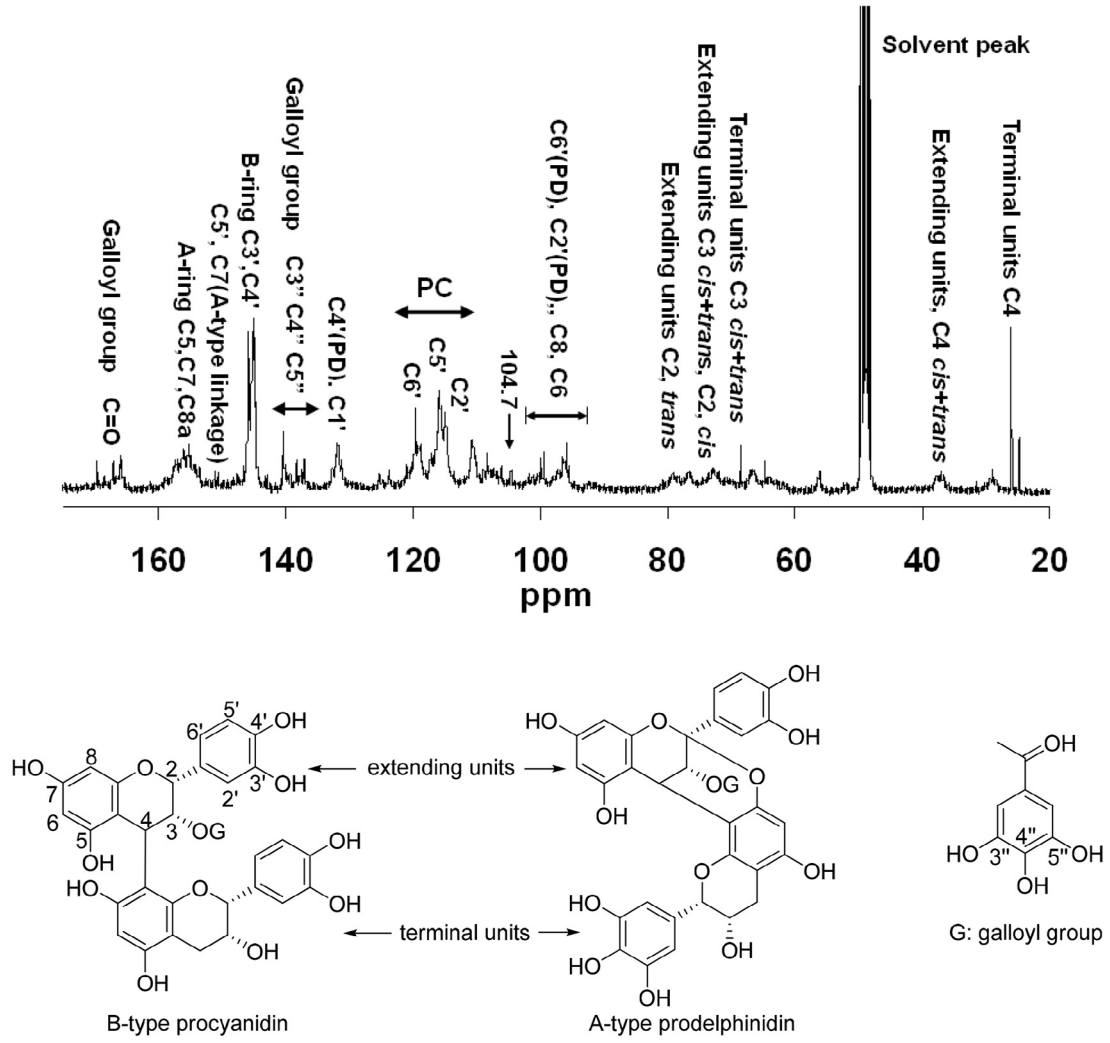

Fig. 3 – ^{13}C NMR spectrum of longan pericarp proanthocyanidins (LPPs) (room temperature, 75 MHz, solvent, CD_3OD). Upper, ^{13}C NMR spectrum; below, typical structures of proanthocyanidins.

Because the detection range imposed by the quadruple analyser in the ESI–MS was from 50 to 2000 Da, the interpretation and quantification of the signals for higher molecular weight proanthocyanidins need stronger tools. Additionally, by ESI–MS method, it is difficult to show the separately charged ions of higher DP proanthocyanidins with a good accuracy (Rodrigues et al., 2007).

To solve these issues, MALDI-TOF–MS was applied. MALDI-TOF–MS is a complementary spectroscopic method which could precisely detect high mass molecules because of the limited production of multiple charged ions. Figure 4B shows the MALDI-TOF–mass spectra of the LPPs recorded as sodium adducts in the positive reflectron ion mode. The periodic occurrence of peak series with distances of 288 Da represented LPPs with different chain lengths; this is consistent with the ^{13}C NMR and ESI–MS spectra. To analyse MALDI-TOF–MS spectra for obtaining the profile of LPPs, an expression of 290 + 288a + 152b + 16c – 2d + 23 was formulated according to the monomeric units and the type of interflavan linkage, where 290 represented the molecular mass of the terminal catechin/epicatechin unit, a was the DP contributed by the extending catechin/epicatechin unit, b was the number of the galloyl group, c was the number of additional hydroxyl group in prodelphenidins, and d was the number of A-type interflavan bond while 23 was the mass of sodium. For example, the peaks at m/z 887 are (epi)catechin trimer with an A-type linkage (887 = 290 + 288*2 – 2*1 + 23). Therefore, these peaks at m/z 887, 1175, 1463, 1751, 2039 and 2327 were attributed to trimeric, tetrameric, pentameric, hexameric, heptameric and octameric PCs with one A-type linkage, respectively. B-type procyanidins trimer, tetramer and pentamer were also observed at m/z 889, 1177, and 1465, respectively. In addition, there were clear mass signals that were 152 Da higher than homoprocyanidins, 2(G) at m/z 1039 to 4(G) at m/z 1615, suggesting the addition of a galloyl group at the heterocyclic C-ring. Therefore, these data clearly revealed in LPPs pure PC polymers and polymer gallates with different ratios of A-type linkage and B-type linkage co-existed. However, consistent with ESI–mass spectra, A-type PC trimer (m/z 863 and 887 in ESI and MALDI-TOF–mass spectra, respectively) was the most abundant molecule. No obvious proanthocyanidin signal after *m*/z 2300 was observed, indicating that LPPs were almost composed of oligomeric

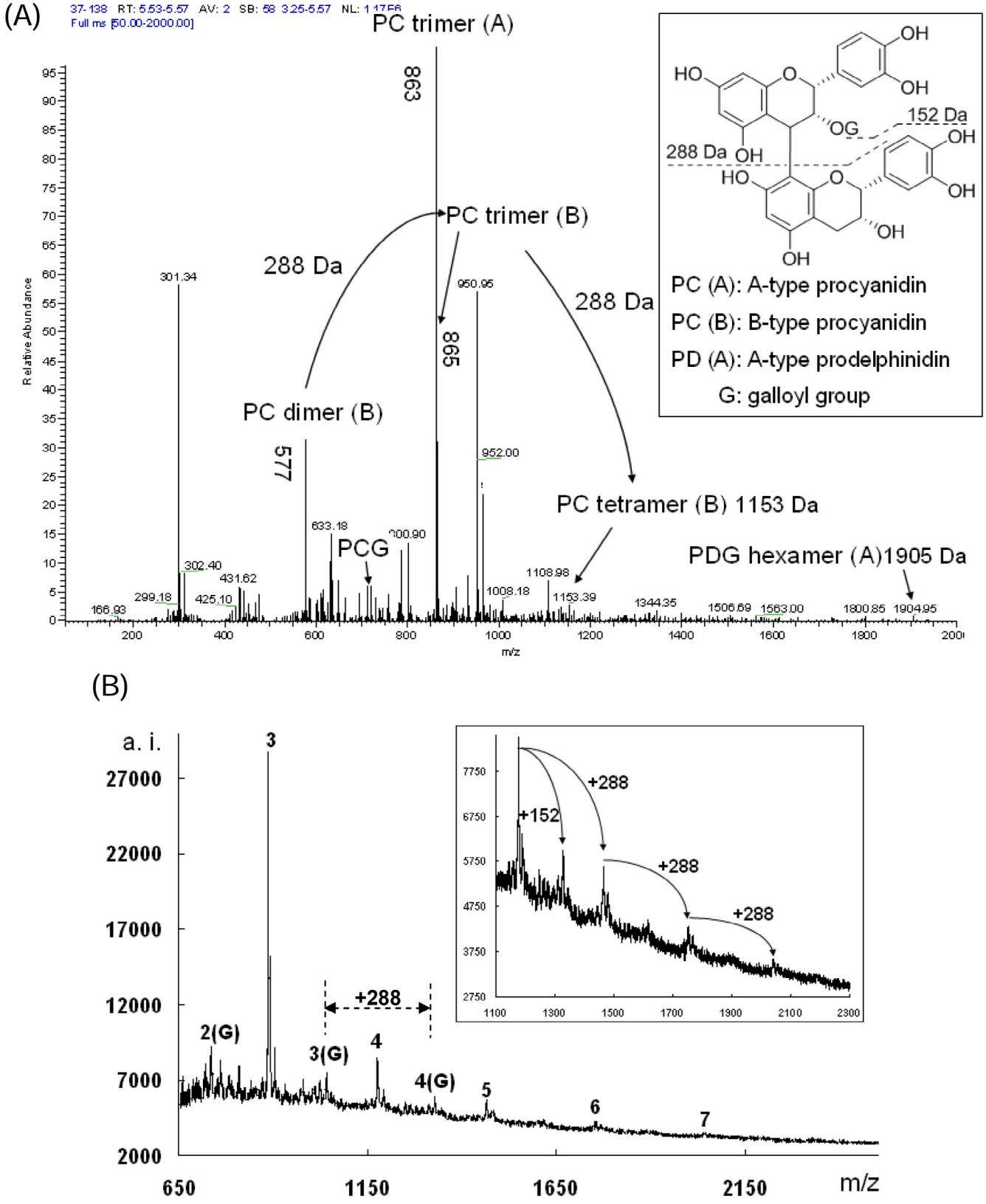

Fig. 4 – ESI and MALDI-TOF mass spectra of longan pericarp proanthocyanidins (LPPs). (A) ESI–MS recorded in the negative ion mode; (B) MALDI-TOF–MS recorded in the $[M + Na]^+$ mode.

proanthocyanidins. This finding is consistent with many proanthocyanidins from other tropical plants (Fu et al., 2007, 2013). ESI and MALDI-TOF–mass spectra clearly showed that A type PC trimer and B-type PC dimer and trimer were the major individual proanthocyanidins. The ratio of individual proanthocyanidins can be approximately calculated according to the peak height of the oligomeric proanthocyanidins in the MALDI-TOF–mass spectra (Fig. 4B) (Krueger, Reed, Feliciano, & Howell, 2013; Yang & Chien, 2000). The yield of dried LPPs was 70 mg per 100 g dry pericarps. Therefore, the contents of A type PC trimer, B-type PC trimer and dimer, and other proanthocyanidins were 33, 13, 9, 15 mg/100 g dry pericarps, respectively.

3.4. *Antioxidant activities of LPPs*

The antioxidant capacity of LPPs was tested by ORAC assay and compared to the commercial proanthocyanidins extracted from grape seed (cGSPs) in order to reveal their potential commercial value. Compared to a Trolox standard, the antioxidant curves of LPPs and cGSPs showed a dose dependent response with a clear lag phase (data not shown). The net area under the kinetic curve changed linearly with concentration of proanthocyanidins. Table 1 shows the ORAC value of LPPs (1.23×10^4 μmol TE/g), which was higher than cGSPs, suggesting LPPs had a potential to be a candidate resembling commercial antioxidant proanthocyanidins. This suggestion was further supported by the report that the ORAC value of commercial pine bark proanthocyanidins being 0.75 μmol TE/g was much lower than that of LPPs (Fu et al., 2007). Therefore, LPPs are a promising alternative for the commercially available proanthocyanidins such as cGSPs and pine bark proanthocyanidins.

3.5. *Inhibitory activities of LPPs against α-amylase*

Since LPPs possess both A-type and B-type PCs, they may have positive effects on glycaemic control. To be sure whether this is true, inhibitory activities of LPPs against α-amylase were investigated. As shown in Fig. 5A, an obvious increase in α-amylase inhibitory activity was observed when concentrations of LPPs increased from 0.025 to 0.5 mg/mL. The percentage inhibition of LPPs was found to be 85.79% at the concentration of 0.5 mg/mL. The IC_{50} value of LPPs against α-amylase was 0.075 ± 0.003 mg/mL (Table 1). These results demonstrated a dose-dependent manner for LPPs against α-amylase and suggested LPPs possessed a strong α-amylase inhibitory activity. Kusano et al. (2011) also demonstrated that acacia bark PCs can effectively inhibit α-amylase and reported an IC_{50} value of 0.068 mg/mL. Similar results were found in the unripe chiku proanthocyanidins, sorghum bicolor bran proanthocyanidins and peanut seed skin proanthocyanidins (Hargrove et al., 2011; Tsujita, Shintani, & Sato, 2014; Wang et al., 2012).

α-Amylase inhibition included reversible or irreversible types depending on specific binding modes and characteristics between enzymes and inhibitors. Figure 5B shows the inhibition kinetics curve of pancreatic α-amylase against LPPs. Compared with the curve in the absence of LPPs ($y = 5.5848x$, $R^2 = 0.9953$), the curve with LPPs had a smaller slope ($y = 4.4357x$, $R^2 = 0.9948$) and passed through the original spot post the addition of LPPs. Because kinetics curve of α-amylase activity by reversible inhibitors showed a straight line starting from the original spot (Yu et al., 2013), therefore, the inhibition type of LPPs against α-amylase was reversible (Hargrove et al., 2011; Kandra, Zajacz, Remenyik, & Gyemant, 2005). To investigate the inhibition mode of the LPPs against pancreatic α-amylase, Lineweaver–Burk plots were generated based on the data generated from enzyme assays (Fig. 5C). When the concentration of LPPs increased, both the slope (s) and the vertical axis intercept (i) increased. Therefore, based on the double-reciprocal

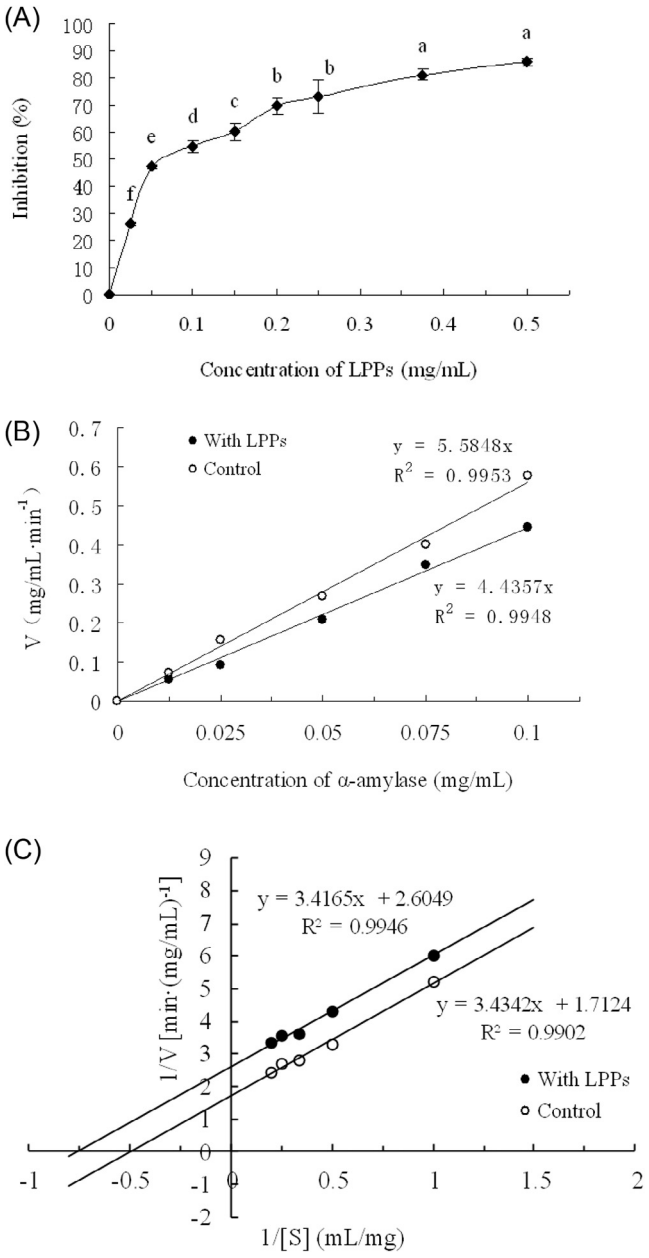

Fig. 5 – Inhibitory activities of longan pericarp proanthocyanidins (LPPs) against α-amylase. (A) Relationship between inhibition ratio and concentration of LPPs; (B) inhibitory kinetics curves of LPPs against α-amylase; (C) Lineweaver–Burk plot for the mode of inhibition of α-amylase by LPPs.

plots of enzyme kinetics (Hargrove et al., 2011), LPPs inhibited α-amylase in uncompetitive mode.

Longan or longan extracts such as LPPs possess health-benefits arising from their components and properties such as antioxidant and α-amylase inhibitory activities. In the current study, the abundance of proanthocyanidins was 26.9 mg/100 g fresh longan pericarps. Though the abundance of LPPs was lower than that of blueberries and whole grains, it was comparable to that of raspberries and greater than many fruits like kiwis, mangoes, avocados and vegetables, indicating the potential commercial value of this fruit byproduct (Gu et al., 2004). LPPs are pretty easy to be processed into powder that can be used as one functional food ingredient. It will be promising to mix longan or LPPs with common staple foods such as wheat flour and rice to slow the starch digestion. Recently, sorghum proanthocyanidins were encapsulated in kafirin microparticles and used as a nutraceutical to successfully inhibit both α-amylase and α-glucosidase during digestion (Links, Taylor, Kruger, & Taylor, 2015), which provided an example for LPPs application. Though the detailed amount needed for having enough significant inhibition on amylase in order to affect physiologically is not clear, the rich abundance of LPPs in addition to corilagin and bioactive polysaccharides that co-existed in longan pericarps suggest that longan pericarps may act as functional food ingredients (Jaitrong et al., 2006; Lei et al., 2014; Prasad et al., 2009; Yang et al., 2009).

The challenges for utilising longan or longan extracts as functional food ingredients are improving their solubility in solvents and sensory properties since polysaccharides in longan pericarps are difficult to dissolve in ethanol while proanthocyanidins and other polyphenols have poor water-solubility. A mixed solution of water and ethanol at proper ratio can help to overcome this challenge when extracting the functional molecules out of longan. For the sensory properties, further tests should be performed.

4. Conclusions

LPPs extracted from longan pericarps and purified by a Sephadex LH-20 column had a final yield of 0.07% based on dry basis. The purity, structure and bioactivity of LPPs were investigated. By UV/vis, FT-IR, ^{1}H and ^{13}C NMR spectra, LPPs oligomers were mainly composed of procyanidin units [catechin and epicatechin] with a mean degree of polymerisation of 3.3. In addition, the ratio of *trans* isomers was approximately equal to that of *cis* isomers in LPPs. These results were further confirmed by ESI–MS and MALDI-TOF–MS spectra, which showed the presence of predominant PC oligomers and a small amount oligomer gallates containing one galloyl group. The successive units in LPPs were coupled each other with abundant both A-type and B-type linkages. Besides, LPPs showed a strong antioxidant activity which is comparable to cGSP products with an ORAC value of 1.23×10^4 μmol TE/g. Moreover, LPPs also inhibited α-amylase in a dose dependent manner under a reversible uncompetitive mode and had an IC_{50} of 0.075 mg/mL, indicating that LPPs possess potentially positive effects on glycaemic control. Overall, these results indicate LPPs mainly consisting of catechin/epicatechin oligomers and are promising to be developed as a functional food component.

Acknowledgements

We thank the financial support by Singapore Ministry of Education Academic Research Fund Tier 1 (R-143-000-583-112) and the start-up grant (R-143-000-561-133) by National University of Singapore. Projects 31371851, 31071617, 31471605 and 31200801 supported by NSFC and Natural Science Foundation of Jiangsu Province (BK20141220) and Fujian Province (Grant No. 2012J05056) also contributed to this research.

REFERENCES

Behrens, A., Maie, N., Knicker, H., & Kögel-Knabner, I. (2003). MALDI-TOF mass spectrometry and PSD fragmentation as means for the analysis of condensed tannins in plant leaves and needles. *Phytochemistry*, *62*(7), 1159–1170.

Chen, X. X., Feng, H. L., Ding, Y. M., Chai, W. M., Xiang, Z. H., Shi, Y., & Chen, Q. X. (2014). Structure characterization of proanthocyanidins from *Caryota ochlandra* Hance and their bioactivities. *Food Chemistry*, *155*, 1–8.

Czochanska, Z., Foo, L. Y., Newman, R. H., & Porter, L. J. (1980). Polymeric proanthocyanidins. Stereochemistry, structural units and molecular weight. *Journal of the Chemical Society-Perkin Transactions*, *1*, 2278–2286.

Foo, L. Y. (1981). Proanthocyanidins: Gross chemical structures by infrared spectra. *Phytochemistry*, *20*(6), 1397–1402.

Fu, C., Loo, A. E., Chia, F. P., & Huang, D. (2007). Oligomeric proanthocyanidins from mangosteen pericarps. *Journal of Agricultural and Food Chemistry*, *55*(19), 7689–7694.

Fu, C., Wang, H., Ng, W., Song, L., & Huang, D. (2013). Antioxidant activity and proanthocyanidin profile of *Selliguea feei* rhizomes. *Molecules*, *18*, 4282–4292.

Gu, L., Kelm, M. A., Hammerstone, J. F., Beecher, G., Holden, J., Haytowitz, D., Gebhardt, S., & Prior, R. L. (2004). Concentrations of proanthocyanidins in common foods and estimations of normal consumption. *The Journal of Nutrition*, *134*(3), 613–617.

Gu, L., Kelm, M. A., Hammerstone, J. F., Beecher, G., Holden, J., Haytowitz, D., & Prior, R. L. (2003). Screening of foods containing proanthocyanidins and their structural characterization using LC/MS/MS and thiolytic degradation. *Journal of Agricultural and Food Chemistry*, *51*(25), 7513–7521.

Guyot, S., Le Guerneve, C., Marnet, N., & Drilleau, J. F. (1999). Methods for determining the degree of polymerization of condensed tannins: A new ^{1}H NMR procedure applied to cider apple procyanidins. In C. G. Gross & T. Yoshida (Eds.), *Plant polyphenols 2: Chemistry, biology, pharmacology, ecology* (pp. 211–222). New York, NY, USA: Kluwer Academic/Plenum Publishers.

Hargrove, J. L., Greenspan, P., Hartle, D. K., & Dowd, C. (2011). Inhibition of aromatase and α-amylase by flavonoids and proanthocyanidins from *Sorghum bicolor* bran extracts. *Journal of Medicinal Food*, *14*(7–8), 799–807.

He, N., Wang, Z. Y., Yang, C. X., Lu, Y. H., Sun, D. H., Wang, Y. P., Shao, W. Y., & Li, Q. B. (2009). Isolation and identification of polyphenolic compounds in longan pericarp. *Separation and Purification Technology*, *70*(2), 219–224.

Huang, D., Ou, B., Hampsch-Woodill, M., & Flanagan, J. (2002). Full automation of oxygen radical absorbance capacity assay on 96-well plate fluorescence reader coupled with multi-channel liquid handling system. *Journal of Agricultural and Food Chemistry*, *50*(16), 4437–4444.

Jaitrong, S., Rattanapanone, N., & Manthey, J. A. (2006). Analysis of the phenolic compounds in longan (*Dimocarpus longan Lour.*) peel. *Proceedings of the Florida State Horticultural Society*, *119*, 371 –375.

Kandra, L., Zajacz, A., Remenyik, J., & Gyemant, G. (2005). Kinetic investigation of a new inhibitor for human salivary alpha-amylase. *Biochemical and Biophysical Research Communications*, *334*(3), 824–828.

Krueger, C. G., Reed, J. D., Feliciano, R. P., & Howell, A. B. (2013). Quantifying and characterizing proanthocyanidins in cranberries in relation to urinary tract health. *Analytical and Bioanalytical Chemistry*, *405*(13), 4385–4395.

Ku, C. S., & Mun, S. P. (2007). Characterization of proanthocyanidin in hot water extract isolated from *Pinus radiata* bark. *Wood Science and Technology*, *41*(3), 235–247.

Kusano, R., Oqawa, S., Matsuo, Y., Tanaka, T., Yazaki, Y., & Kouno, I. (2011). α-Amylase and lipase inhibitory activity and structural characterization of acacia bark proanthocyanidins. *Journal of Natural Products*, *74*(2), 119–128.

Lei, Y., Ren, X., Chen, J., Liu, D., & Ruan, J. (2014). Protective effects of grape seed-derived procyanidin extract against carrageenan-induced abacterial prostatitis in rats. *Journal of Functional Foods*, *7*, 416–424.

Links, M. R., Taylor, J., Kruger, M. C., & Taylor, J. R. N. (2015). Sorghum condensed tannins encapsulated in kafirin microparticles as a nutraceutical for inhibition of amylases during digestion to attenuate hyperglycaemia. *Journal of Functional Foods*, *12*, 55–63.

Nagahama, K., Eto, N., Sakakibara, Y., Matsusita, Y., Sugamoto, K., Morishita, K., & Suiko, M. (2014). Oligomeric proanthocyanidins from rabbiteye blueberry leaves inhibits the proliferation of human T-cell lymphotropic virus type 1-associated cell lines via apoptosis and cell cycle arrest. *Journal of Functional Foods*, *6*, 356–366.

Neto, C. C. (2007). Cranberry and its phytochemicals: A review of *in vitro* anticancer studies. *The Journal of Nutrition*, *137*(s1), 186S–193S.

Ou, K. Q., & Gu, L. W. (2014). Absorption and metabolism of proanthocyanidins. *Journal of Functional Foods*, *7*, 43–53.

Panyathep, A., Chewonarin, T., Taneyhill, K., Surh, Y., & Vinitketkumnuen, U. (2013). Effects of dried longan seed (*Euphoria longana* Lam.) extract on VEGF secretion and expression in colon cancer cells and angiogenesis in human umbilical vein endothelial cells. *Journal of Functional Foods*, 5(3), 1088–1096.

Prasad, K. N., Yang, B., Zhao, M., Sun, J., Wei, X., & Jiang, Y. (2010). Effects of high pressure or ultrasonic treatment on extraction yield and antioxidant activity of pericarp tissues of longan fruit. *Journal of Food Biochemistry*, *34*(4), 838–855.

Prasad, K. N., Yang, B., Zhao, M., Wei, X., Jiang, Y., & Chen, F. (2009). High pressure extraction of corilagin from longan (*Dimocarpus longan* Lour.) fruit pericarp. *Separation and Purification Technology*, *70*(1), 41 –45.

Ranilla, L. G., Kwon, Y. I., Apostolidis, E., & Shetty, K. (2010). Phenolic compounds, antioxidant activity and *in vitro* inhibitory potential against key enzymes relevant for hyperglycemia and hypertension of commonly used medicinal plant, herbs and spices in Latin America. *Bioresource Technology*, *101*(12), 4676–4689.

Rodrigues, C. M., Rinaldo, D., dos Santos, L. C., Montoro, P., Piacente, S., Pizza, C., Hiruma-Lima, C. A., Souza Brito, A. R. M., & Vilegas, W. (2007). Metabolic fingerprinting using direct flow injection electrospray ionization tandem mass spectrometry for the characterization of proanthocyanidins from the barks of *Hancornia speciosa*. *Rapid Communications in Mass Spectrometry*, *21*(12), 1907–1914.

Seiler, N., Chaabi, M., Roussi, S., Gosse, F., Lobstein, A., & Raul, F. (2006). Synergism between apple procyanidins and lysosomotropic drugs: Potential in chemoprevention. *Anticancer Research*, *26*(5A), 3381–3385.

Shao, Z. H., Vanden Hoek, T. L., Li, C. Q., Schumacker, P. T., Becker, L. B., Chan, K. C., Qin, Y., Yin, J. J., & Yuan, C. S. (2004). Synergistic effect of *Scutellaria baicalensis* and grape seed proanthocyanidins on scavenging reactive oxygen species *in vitro*. *American Journal of Chinese Medicine*, *32*(1), 89–95.

Tsujita, T., Shintani, T., & Sato, H. (2014). Preparation and characterization of peanut seed skin polyphenols. *Food Chemistry*, *151*, 15–20.

Wang, H., Liu, T., Song, L., & Huang, D. (2012). Profiles and α-amylase inhibition activity of proanthocyanidins in unripe *Manilkara zapota* (Chiku). *Journal of Agricultural and Food Chemistry*, *60*(12), 3098–3104.

Wangensteen, H., Bräunlich, M., Nikolic, V., Malterud, K. E., Slimestad, R., & Barsett, H. (2014). Anthocyanins, proanthocyanidins and total phenolics in four cultivars of aronia: Antioxidant and enzyme inhibitory effects. *Journal of Functional Foods*, *7*, 746–752.

Xu, S., Zou, B., Yang, J., Yao, P., & Li, C. (2012). Characterization of a highly polymeric proanthocyanidin fraction from persimmon pulp with strong Chinese cobra PLA2 inhibition effects. *Fitoterapia*, *83*(1), 153–160.

Yang, B., Jiang, Y., Shi, J., Chen, F., & Ashraf, M. (2011). Extraction and pharmacological properties of bioactive compounds from longan (*Dimocarpus longan* Lour.) fruit - A review. *Food Research International*, *44*(7), 1837–1842.

Yang, B., Zhao, M., & Jiang, Y. (2009). Anti-glycated activity of polysaccharides of longan (*Dimocarpus longan* Lour.) fruit pericarp treated by ultrasonic wave. *Food Chemistry*, *114*(2), 629–633.

Yang, Y., & Chien, M. (2000). Characterization of grape procyanidins using high-performance liquid chromatography/mass spectrometry and matrix-assisted laser desorption/ionization time-of-flight mass spectrometry. *Journal of Agricultural and Food Chemistry*, *48*(9), 3990–3996.

Yazaki, Y., & Hillis, W. E. (1977). Polyphenolic extractives of *Pinus radiata* bark. *Holzforschung*, *31*(1), 20–25.

Yu, Y., Gao, F., Deng, X., Pu, X., Zhang, M., & Pang, Y. (2013). Inhibitory effect of polyphenol extracts from peanut shells on the activity of pancreatic α-amylase activity *in vitro*. *Journal of Food Agriculture & Environment*, *11*(2), 38–42.

Zhou, H. C., Lin, Y. M., Wei, S. D., & Tam, N. F. Y. (2011). Structural diversity and antioxidant activity of condensed tannins fractionated from mangosteen pericarp. *Food Chemistry*, *129*(4), 1710–1720.

Zou, B., Nie, R., Zeng, J., Ge, Z., Xu, Z., & Li, C. (2014). Persimmon tannin alleviates hepatic steatosis in L02 cells by targeting miR-122 and miR-33b and its effects closely associated with the A type ECG dimer and EGCG dimer structural units. *Journal of Functional Foods*, *11*, 330–341.